Distribution of Nanoparticles in Lamellar Domains of Block Copolymers

Julia J. Chiu,[†] Bumjoon J. Kim,[†] Gi-Ra Yi,[†] Joona Bang,[‡,§] Edward J. Kramer,[†,‡] and David J. Pine*[,†,‡,⊥]

Department of Chemical Engineering and Department of Materials, University of California, Santa Barbara, Santa Barbara, California 93106, and Nano-Bio System Research Team, Seoul Center, Korea Basic Science Institute, Seoul 136-713, Republic of Korea

Received July 5, 2006; Revised Manuscript Received February 8, 2007

ABSTRACT: Polystyrene-coated gold nanoparticles (molecular weight (M_n) of PS ~1300 g/mol, average particle diameter d (core + shell) ~ 9.2 ± 2.2 nm, corresponding to a high areal chain density of PS) are incorporated into symmetric poly(styrene-*b*-2 vinylpyridine) diblock copolymers with total M_n ~ 60 000−380 000 g/mol at volume fractions of 0.07−0.32. For all M_n of diblock copolymers and particle filling fractions examined, particles are centralized in the PS domains with Gaussian distribution profiles. The distribution width generally decreases as the PS domain size decreases or as the particle weight fraction increases. These observations are discussed in terms of the relative entropic contributions of the polymer chains and particles.

Introduction

Self-assembly of inorganic nanoparticles in block copolymer thin films has attracted much attention due to its ability to control and direct structure at the nanometer length scale. Recent reports have shown some success in directed self-assembly of particles within block copolymer templates. These studies include deposition of particles formed in situ within the desired block copolymer domains[1−4] as well as controlled placement of particles formed ex situ using block copolymer templates.[5−10] Nevertheless, detailed experimental studies exploring many of the important factors that control the location and assembly of particles within the respective block copolymer domains have not been reported. Recent calculations[11,12] suggest that the location of particles within a block copolymer domain can be controlled simply by varying the size d of the particles relative to the size L of the polymer domain in which they reside. The particle filling fraction is also predicted to play an important role in particle self-assembly.[11,13]

In this article, we investigate the self-assembly of particles within block copolymer matrices and study the effects of particle size and particle filling fraction on particle assembly. The system we devise consists of nanoparticles formed ex situ and then introduced into symmetric diblock copolymer templates for which the d/L ratio and particle weight fraction are varied. Entropic contributions to the free energy, as well as enthalpic differences between the surface of the particles and the polymer matrix, influence where the particles reside.[14] In order to minimize the role of enthalpy on particle location within a polymer domain, we functionalize the particles with short homopolymers A and disperse them in an A−B diblock copolymer matrix, thus ensuring that the interaction between the particles and the A block is minimized. As might be expected, we find that particles are confined to the A block. We then investigate localization of particles within the A block for various d/L ratios by varying the molecular weight (M_n) of the symmetric diblock copolymer, thereby varying L while keeping the particle size d unchanged. In a parallel set of experiments using the same size of particles and molecular weight of diblock copolymer template, we also investigate localization of particles for various particle concentrations by controlling the concentration of particles at fixed M_n.

* To whom correspondence should be addressed. E-mail: pine@nyu.edu.
[†] Department of Chemical Engineering, UC Santa Barbara.
[‡] Department of Materials, UC Santa Barbara.
[§] Korea University.
[⊥] Present address: Department of Physics, New York University, 4 Washington Place, New York, NY 10003.

Experimental Details

We use gold nanoparticles functionalized with thiol-terminated polystyrene (PS) chains and symmetric poly(styrene-*b*-2 vinylpyridine) (PS−P2VP) copolymers with total M_n ranging from 60 000 to 400 000 g/mol and low polydispersities ($M_w/M_n \leq 1.11$). The properties of each diblock copolymer are listed in Table 1. PS−P2VP with M_n = 60,000 is synthesized by living anionic polymerization and other copolymers are purchased from Polymer Source, Inc. (Montreal, Canada). Thiol-terminated PS chains (M_n ~ 1300 g/mol, M_w/M_n = 1.10) are synthesized by living anionic polymerization of styrene followed by reaction of the polyanion with propylene sulfide.[15] The molecular weight of the thiol-terminated PS chains is determined by GPC and confirmed by NMR end-group analysis. Gold particles functionalized with thiol-terminated PS chains are synthesized by a two-phase method[16] with a Au/S ratio of 1.0 via the reduction of $HAuCl_4 \cdot 3H_2O$ by sodium borohydride in the presence of thiol-terminated PS stabilizing chains dissolved in toluene. Particles are dried from toluene and washed with a toluene/methanol mixture to remove any residual reducing and transfer agents and unbound thiols.

To prepare the polymer−nanoparticle composite, we typically prepare a 2 wt % polymer solution in dichloromethane, a nonselective solvent for PS and P2VP, admixed with PS-coated gold particles having a weight fraction of ~0.2 in the solid (which corresponds to 0.15 in volume fraction of gold and PS thiol in the total polymer matrix). A polymer−particle composite film is prepared by solvent casting a mixture of nanoparticles and polymer in dichloromethane onto an epoxy substrate and then annealing under a saturated solvent atmosphere at 25 °C. The solvent annealing time is usually 1 day followed by 1 day of slow drying in air. Subsequent removal of any residual solvent is done under vacuum for a minimum of 4 h. The resulting film consists of alternating PS and P2VP lamellar layers parallel to the film−air interface with the top layer being PS because the PS/air interfacial energy is lower than that of P2VP/air.[17] Gold particle location with

10.1021/ma061503d CCC: $37.00
Published on Web 03/21/2007

Table 1. Properties of Various Diblock Copolymers Used for Samples with Varying *d*/*L* Ratios

sample	M_n, g/mol	PS fraction, %	M_w/M_n	L_{PS}, nm	*d*/*L*
A	60 000	52.0	1.05	21	0.44
B	114 500	50.0	1.08	30	0.31
C	196 500	46.6	1.11	52	0.18
D	380 000	50.0	1.10	71	0.13

respect to lamellar domain boundaries is determined by cross-sectional transmission electron microscopy (TEM) performed on a FEI T20 microscope operated at 200 kV. For these analyses, samples are prepared by microtoming epoxy-supported bulk films and by subsequent selective staining of the P2VP domains using iodine vapor. The lamellar periods of the neat polymers are estimated by small-angle X-ray scattering (SAXS) and dynamic secondary ion mass spectroscopy (DSIMS). SAXS measurements are done on bulk polymer films while DSIMS profiles are obtained for silicon wafer-supported thin film samples annealed at the same temperature (200 °C). A thin (~200 nm) silicon dioxide layer is deposited on the neat wafer prior to use.

The particle size distribution of the gold is determined using TEM. A monolayer of particles is prepared by drying a drop of dilute gold suspension placed on a thin carbon substrate supported by a copper grid. The size distribution is obtained from TEM images of at least 400 particles using standard image analysis software. The gold core diameter distribution obtained as a histogram from the TEM image analysis was used to calculate the average surface area per gold nanoparticle. Weight fractions of gold and polymer chains were measured by thermal gravimetric analysis (TGA). These numbers were confirmed by elemental analysis. The weight fractions of carbon, hydrogen, and nitrogen in polymer-coated Au particles were measured, and the weight fraction of residue was assumed to be that of the gold core. The weight fractions of the polymer chains were converted into volume fractions using the density of the polymer (~1.05 g/cm^3) and the density of the gold particles (~19.3 g/cm^3). The number of polymer chains per each gold particle for various core−shell type particles, divided by the average surface area of the gold particle, gives the chain areal density of polymer chains on the particle surface.

Results

The average particle core (Au) diameter measured is 2.5 ± 0.8 nm (see histogram in Figure 1). The diameter of the particles *d* (core + shell), which is estimated from the center-to-center distance between particles, is approximately 9.2 ± 2.2 nm. Thus, the average polymer shell thickness is 3.4 nm. These estimates of core and shell thicknesses yield gold and polymer weight fractions that are in good agreement with elemental analysis data obtained for these PS-coated gold nanoparticles. The areal chain density of PS chains on the gold particle surface is ~9.3 chains/nm^2. This areal chain density is sufficiently high to prevent the contact of the gold surface of partially covered gold particles with the P2VP block chains, contact that has been shown to cause the gold particles to bind to the PS−P2VP interface.[18] For PS-thiols of M_n = 1.5 kg/mol such interfacial segregation occurs below an areal chain density of ~2.5 chains/nm^2.[19] The respective PS domain sizes (L_{PS}) for PS−P2VP diblock copolymer with various molecular weights obtained from SAXS and DSIMS are also in good agreement and are summarized in Table 1. Using these values and the average *d* (core + shell) of 9.2 ± 2.2 nm, the corresponding *d*/*L* ratios are also listed.

Using PS−P2VP with M_n in the range 60 000−380 000 g/mol, four samples with *d*/*L* ratios ranging from 0.44 to 0.13 are prepared at a fixed particle volume fraction of 0.15, as summarized in Table 1. TEM images obtained for each sample are shown in Figure 2. Gold particles, appearing as dark spots in bright field TEM, are found at or near the center of the PS block (unstained) for all samples while P2VP domains (stained) are completely free of particles. The absence of particles in the P2VP domains is checked by TEM analysis of unstained samples.

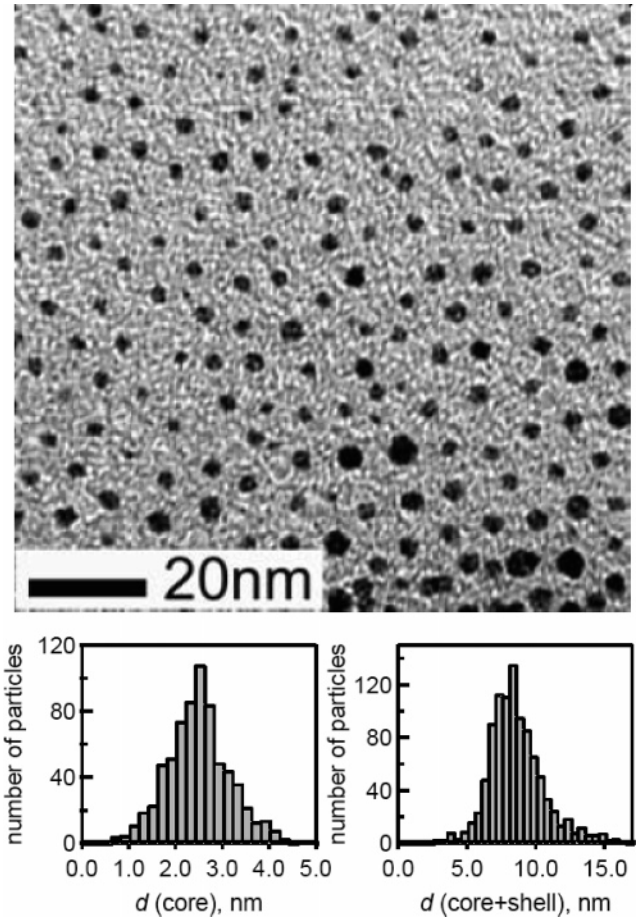

Figure 1. TEM image of PS-coated gold nanoparticles and the corresponding histograms of size distribution for *d* (core) and *d* (core + shell) with averages of 2.5 ± 0.8 and 9.2 ± 2.2 nm, respectively.

The distribution of particle locations within the PS block is obtained for each sample by detailed image analysis. Figure 3 shows histograms of particle location plotted as the normalized distance from the center of the domain for various *d*/*L* ratios. As illustrated, the particle distributions fitted to Gaussian profiles (solid lines) show particle concentration being the highest at the center of the PS domain (0 on the normalized *x*-axis) and falling to zero at the interfaces (±1 on the *x*-axis) between the PS and P2VP blocks. In particular, the normalized width of the distribution σ/L is larger for the larger molecular weight polymers ($\sigma/L \sim 0.50$ and 0.53 for 196 500 and 400 000 g/mol, respectively) compared to the smaller diblock copolymers ($\sigma/L \sim 0.40$ and 0.36 for molecular weights 60 000 and 114 500 g/mol, respectively). We do not observe any segregation of particles according to particle size; particles are randomly distributed around the center of the PS domains irrespective of their diameter.

As the filling fraction of gold particles in the diblock copolymer matrix is varied, changes in the particle distribution are also observed at a fixed *d*/*L*. Using PS−P2VP with $M_n \sim$ 196 000 g/mol (*d*/*L* = 0.18), cross-sectional TEM images and particle distribution proflies for particle/polymer composite films prepared with particle volume fractions ranging from 0.07 to 0.32 (0.1−0.4 in weight fractions) are obtained and shown in Figures 4 and 5, respectively. Higher volume fractions lead to

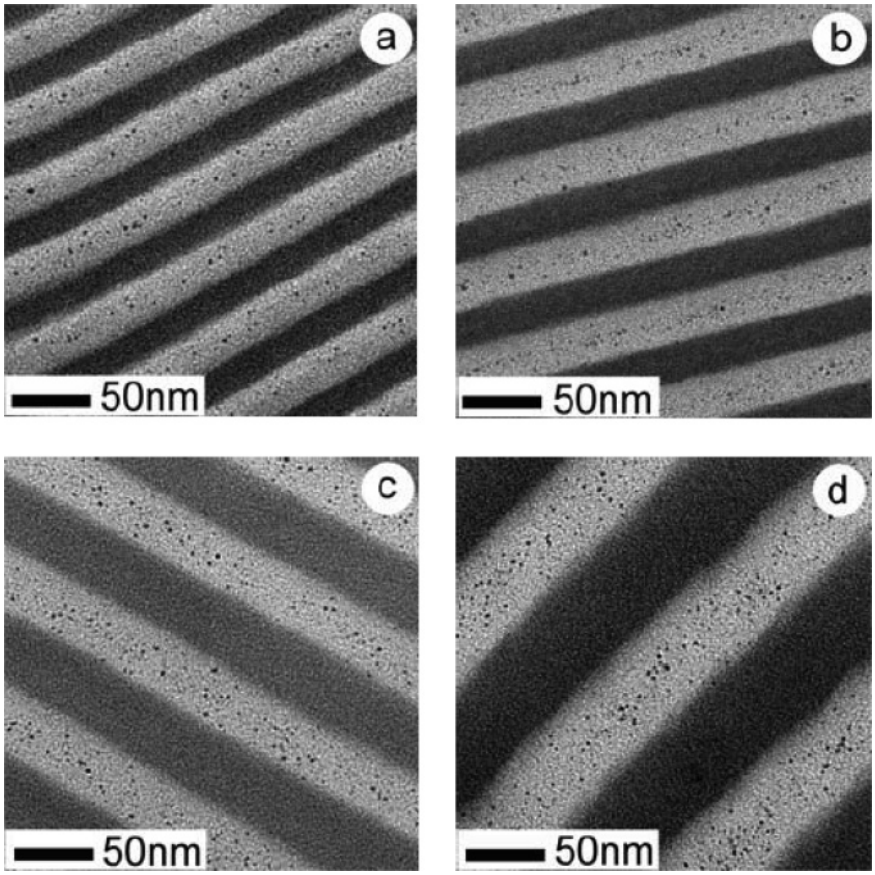

Figure 2. Cross-sectional TEM images of gold/block copolymer composite films of PS−P2VP with various molecular weights (total M_n): (a) 60, (b) 114.5, (c) 196.5, and (d) 380 kg/mol. Particle volume fraction (core + shell) is ∼0.15.

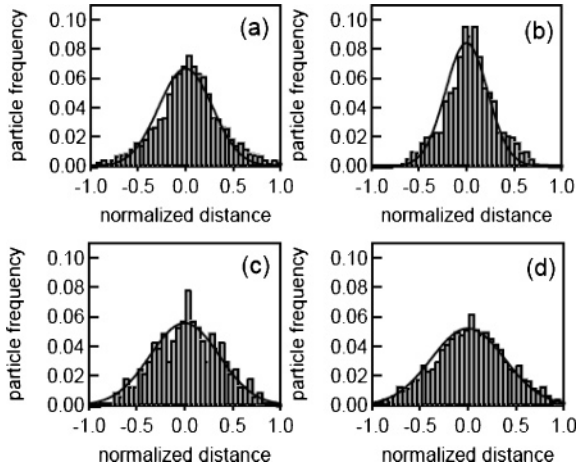

Figure 3. Corresponding histograms of the particle distribution as a function of normalized distance from the center of the PS domain for the samples shown in Figure 2.

macrophase separation of regions of a PS-coated gold particle phase from the particle containing block copolymer.[19] Similar to our observations above, the particle concentration profiles for all samples exhibit Gaussian distributions where the particle concentration is highest at the center of the PS domain. Furthermore, the width of the Gaussian distribution ($\sigma/L \sim 0.57$, 0.50, 0.39, and 0.30, which corresponds to volume fractions of 0.07, 0.15, 0.23, and 0.32, respectively) decreases as the filling fraction of particles increases, as shown in Figure 5 and summarized in Figure 6. For the image shown in Figure 4b, roughly 70% of all gold particles can be found within ∼5 nm from the center line of the PS domains. This corresponds to approximately the middle 20% of the domain.

Discussion

The self-assembly of nanoparticles near the center of the particle-compatible block copolymer lamellar domain that we observe is generally consistent with recent numerical calculations by Balazs et al.[11,12] For brevity, we revert to referring to the particle-compatible and incompatible domains as the "A" and "B" domains, respectively. The calculations of Balazs et al. predict that the positions of nanoparticles are localized around the center of the A domain if the particles are large compared to the domain size, i.e., when $d/L \geq 0.3$. When d/L is smaller, the calculations predict that the particles remain entirely within the A domain but move outward toward the edges of the domain so that the concentration of particles is lower at the center of the domain than near its edges. These two cases are referred to as the *center-filled* and *edge-filled* lamellar phases, respectively. In our experiments, we observe only the centered-filled morphology, irrespective of the value of d/L; the particle density is largest at the center of the A domain for all values of d/L ranging from 0.13 to 0.44, evidenced by the location of the peaks of particle frequency in the distribution profiles shown in Figure 5. It is important to note, however, that the nanoparticles we use are fairly polydisperse, with diameters of 9.2 ± 2.2 nm. Moreover, the outer layer of our particles consists of a dense polymer brush. By contrast, the numerical calculations assume perfectly monodisperse hard-sphere particles. These are important differences that very well may affect the ordering of particles within the A domain.

While we do not observe the edge-filled morphology in our experiments, we do observe a tendency for the particles to become more delocalized within the A domain as d/L decreases. This general tendency can be understood within the context of the numerical calculations of Balazs et al. Their calculations

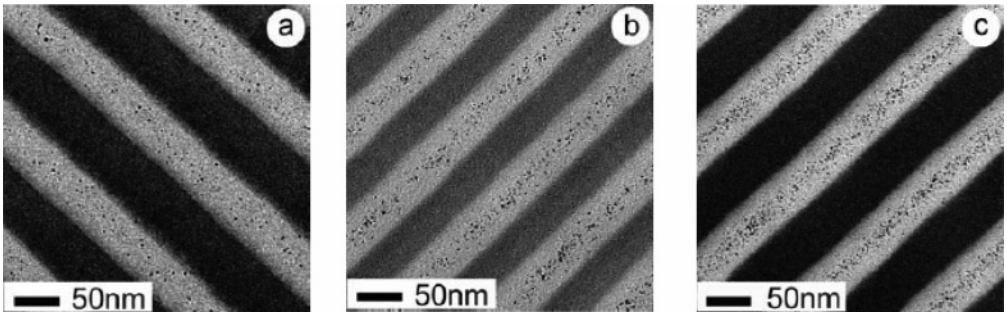

Figure 4. Cross-sectional TEM images of gold/block copolymer composite films with particle volume fractions (core + shell) of (a) 0.07, (b) 0.23, and (c) 0.32. TEM for the sample prepared with particle volume fraction of 0.15 is displayed in Figure 2c. Molecular weight (M_n) of the PS−P2VP copolymer is ~196.5 kg/mol.

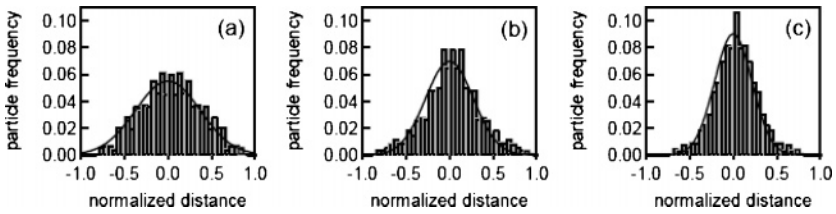

Figure 5. Corresponding histograms of the particle distribution as a function of normalized distance from the center of the PS domain for the samples shown in Figure 4.

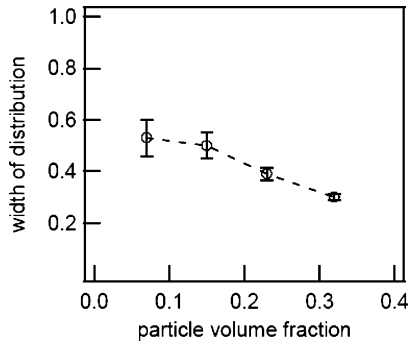

Figure 6. Width of the Gaussian particle distribution for various filling fractions.

predict that the entropic cost of stretching the A polymer chains in order to accommodate the particles is greater than can be offset by the translational entropy of the particles, which is maximized by distributing particles homogenously throughout the domain. To avoid this large stretching penalty, the translational entropy of the particles is sacrificed by localizing particles at the narrow regions near the center of the polymer domains where the ends of the polymer chains are located. In this way, chain stretching can be almost completely avoided by opening up space for the particles between the ends of the A blocks at the center of the A domain. This interpretation of the entropic contribution to the free energy is consistent with our observation that the center-filled morphology is found for all samples prepared with particle volume fractions up to 0.32 and d/L ratios from 0.13 to 0.44. As d/L decreases, the chain stretching penalty is lessened, and the particles are less likely to be confined to the center of the polymer domains, consistent with our observation that particles are more dispersed as the block copolymer domain size increases.

When the particle concentration is increased at fixed d/L, the distribution of particles around the center of the A domain becomes narrower, as summarized by the data in Figure 6. The mean-field theory simulations of particle/block copolymer hybrid materials[11] predict that as the filling fraction of particles increases, the particles organize cooperatively to form a well-ordered self-assembled (SA) core−shell structure in which a tightly packed particle core is surrounded by a diblock copolymer shell. For our system, formation of such well-ordered SA phase is hindered by the polydispersity of particles; instead, particles simply pack more densely around the center of the PS domains, as evidenced by the particle distribution profiles. To understand these observations, we refer again to the relative entropic contributions of the particles and diblock copolymer chains. As the particle filling fraction increases in a diblock copolymer matrix, dispersion of particles within the PS domain becomes increasingly unfavorable as the PS chains must stretch farther to accommodate more particles. This increase in stretching penalty cannot be offset by particle translational entropy, and thus particles are prevented from spreading throughout the PS domains. To accommodate higher volume of particles without incurring a larger stretching penalty, more particles localize near the center of the compatible PS domains. As a result, the width of the particle distribution in the PS domain profile narrows as the filling fraction increases.

We can gain insight by comparing our particle/block copolymer system with homopolymer A and A−B diblock copolymer blends, which have been studied extensively.[20−26] It was observed that for systems consisting of homopolymers completely solubilized in the diblock copolymer matrix[20,23,24] (i.e., for the case where no macroscopic phase separation between the two polymers occurs) low-M_n homopolymers are distributed throughout the compatible polymer domain with nearly uniform swelling of the block while high-M_n homopolymers accumulate at the center of the respective lamellar domains. For such binary blend of homopolymer and diblock copolymer, the distribution profile of homopolymers changes gradually from central to nearly homogeneous as M_n of the homopolymer decreases.

Similarly, for our particle/block copolymer system, particles gradually change from a center-segregated state to a more dispersed state as the polymer domain size increases (d/L decreases) as indicated by the width of the Gaussian particle distribution which increases as the molecular weight of the PS−P2VP diblock copolymer template increases. A recent report[27] involving PS-coated gold particles dispersed in poly(styrene-*b*-ethylene propylene) (PS−PEP) copolymer with small d/L ratio of 0.045 showed a homogeneous distribution of particles within

the PS polymer domain. Such a particle distribution is expected for our system in the limit of $d/L \ll 1$. Thus, our particles in PS−P2VP templates appear like homopolymers PS with intermediate molecular weights that swell the PS domains nonuniformly by locating around the center of the respective domains in the polymer matrix.

To fully understand of the results presented here, a better understanding concerning at what stage in the processing the final distribution of particles is formed may be needed. During the formation process, we have a three-component system comprised of block copolymer, polymer-coated particles, and solvent. The morphology we observe for the solvent-annealed samples reflects the equilibrium structure when the glass transition temperature of the system is approximately room temperature as the solvent slowly evaporates, and it corresponds to the point where 15−25 vol % solvent remains.[28] While we feel confident that the structure with this small an amount of the nonpreferential solvent dichloromethane is close to the equilibrium state for the two-component system, it would be nice to verify this hypothesis by annealing above the glass-transition temperature of the polymer. Unfortunately, we are prevented from doing so because the thiol-bound PS dissociates from the gold particles very near the glass transition temperature for PS.

The particles we use are polymer coated metal particles whose interactions may not be sufficiently described by those of hard spheres. As mentioned, the particles also consist of a finite size distribution which may further contribute to particle assembly that is different from that predicted for model monosize spheres. While there exist models for binary systems that describe the equilibrium morphology and distribution of homopolymers or hard spheres in diblock copolymer matrices in sufficient detail,[11,13,24,29] a realistic model that includes solvent effects as well as polymer-coated spheres with a finite size distribution may be needed to describe fully the self-assembly process that takes place here in our experiments.

Summary

We have designed an experimental system consisting of diblock copolymer and nanoparticles whose surfaces are modified to be enthapically similar to one of the blocks. This system is used to investigate particle arrangement within well-ordered block copolymer domains due to entropic effects while enthalpic contributions are minimized or can be ignored. For 100% PS-coated particles dispersed in PS−P2VP diblock copolymer with particle volume fractions ranging from 0.07 to 0.32, particle segregation toward the center of the PS domain is observed for all volume fractions with a decrease in the distribution width as the particle volume fraction increases. Particle location at d/L ratios ranging from 0.13 to 0.44 is also investigated using different molecular weights of diblock copolymers. The results are interpreted in terms of the relative entropic contributions of the particles and the diblock copolymers and are compared with recent theoretical calculations based on similar systems. For low molecular weight diblocks, PS-coated gold nanoparticles resides at or near the center of the PS domain as predicted. For high molecular weight diblocks, particles are less confined to the center as predicted and are evidenced by a broader distribution in our experiments. To understand precisely the behavior of polymer-coated particles within diblock copolymer templates at various d/L ratios and weight fractions, a realistic model that captures the essential features of the three-component experimental system that includes polymer-coated particles, block copolymer, and solvent used here is needed.

Acknowledgment. This work was supported in part by the US Department of Energy under Award DE-F602-02ER45998 and the MRSEC Program of the National Science Foundation under Award DMR05-20415. This work made use of Central Facilities of the UCSB Materials Research Laboratory supported by the US NSF under Award DMR05-20415. We gratefully acknowledge Dr. Kurt Knipmeyer for help with image analysis.

References and Notes

(1) Morkved, T. L.; Wiltzius, P.; Jaeger, H. M.; Grier, D. G.; Witten, T. A. *Appl. Phys. Lett.* **1994**, *64*, 422−424.
(2) Bronstein, L. H.; Sidorov, S. N.; Valetsky, P. M.; Hartmann, J.; Colfen, H.; Antonietti, M. *Langmuir* **1999**, *15*, 6256−6262.
(3) Horiuchi, S.; Sarwar, M. I.; Nakao, Y. *Adv. Mater.* **2000**, *12*, 1507−1511.
(4) Lopes, W. A.; Jaeger, H. M. *Nature (London)* **2001**, *414*, 735−738.
(5) Lauter-Pasyuk, V.; Lauter, H. J.; Ausserre, D.; Gallot, Y.; Cabuil, V.; Kornilov, E. I.; Hamdoun, B. *Physica B* **1997**, *241*, 1092−1094.
(6) Zehner, R. W.; Lopes, W. A.; Morkved, T. L.; Jaeger, H.; Sita, L. R. *Langmuir* **1998**, *14*, 241−244.
(7) Tsutsumi, K.; Funaki, Y.; Hirokawa, Y.; Hashimoto, T. *Langmuir* **1999**, *15*, 5200−5203.
(8) Bockstaller, M.; Kolb, R.; Thomas, E. L. *Adv. Mater.* **2001**, *13*, 1783−1786.
(9) Bockstaller, M. R.; Lapetnikov, Y.; Margel, S.; Thomas, E. L. *J. Am. Chem. Soc.* **2003**, *125*, 5276−5277.
(10) Zhang, C. L.; Xu, T.; Butterfield, D.; Misner, M. J.; Ryu, D. Y.; Emrick, T.; Russell, T. P. *Nano Lett.* **2005**, *5*, 357−361.
(11) Thompson, R. B.; Ginzburg, V. V.; Matsen, M. W.; Balazs, A. C. *Science* **2001**, *292*, 2469−2472.
(12) Thompson, R. B.; Ginzburg, V. V.; Matsen, M. W.; Balazs, A. C. *Macromolecules* **2002**, *35*, 1060−1071.
(13) Huh, J.; Ginzburg, V. V.; Balazs, A. C. *Macromolecules* **2000**, *33*, 8085−8096.
(14) Chiu, J. J.; Kim, B. J.; Kramer, E. J.; Pine, D. J. *J. Am. Chem. Soc.* **2005**, *127*, 5036−5037.
(15) Stouffer, J. M.; McCarthy, T. J. *Macromolecules* **1988**, *21*, 1204−1208.
(16) Brust, M.; Walker, M.; Bethell, D.; Schiffrin, D. J.; Whyman, R. *J. Chem. Soc., Chem. Commun.* **1994**, 801−802.
(17) Kim, B. J.; Chiu, J. J.; Yi, G.-R.; Pine, D. J.; Kramer, E. J. *Adv. Mater.* **2005**, *17*, 2618−2622.
(18) Kim, B. J.; Bang, J.; Hawker, C. J.; Kramer, E. J. *Macromolecules* **2006**, *39*, 4108−4114.
(19) Kim, B. J.; Kramer, E. J. Manuscript in preparation.
(20) Hashimoto, T.; Tanaka, H.; Hasegawa, H. *Macromolecules* **1990**, *23*, 4378−4386.
(21) Tanaka, H.; Hasegawa, H.; Hashimoto, T. *Macromolecules* **1991**, *24*, 240−251.
(22) Winey, K. I.; Thomas, E. L.; Fetters, L. J. *Macromolecules* **1991**, *24*, 6182−6188.
(23) Mayes, A. M.; Russell, T. P.; Satija, S. K.; Majkrzak, C. F. *Macromolecules* **1992**, *25*, 6523−6531.
(24) Shull, K. R.; Winey, K. I. *Macromolecules* **1992**, *25*, 2637−2644.
(25) Matsushita, Y.; Torikai, N.; Mogi, Y.; Noda, I.; Han, C. C. *Macromolecules* **1993**, *26*, 6346−6349.
(26) Hasegawa, H.; Hashimoto, T. *Self-Assembly and Morphology of Block Copolymer Systems*; Pergamon: London, 1996.
(27) Bockstaller, M. R.; Thomas, E. L. *Phys. Rev. Lett.* **2004**, *93*, 166106.
(28) Kambour, R. P.; Gruner, C. L.; Romagosa, E. E. *J. Polym. Sci., Polym. Phys.* **1973**, *11*, 1879−1890.
(29) Sides, S. W.; Kim, B. J.; Kramer, E. J.; Fredrickson, G. H. *Phys. Rev. Lett.* **2006**, *96*, 250601−4.

MA061503D